RSC Advances

PAPER

View Article Online
View Journal | View Issue

Cite this: *RSC Adv.*, 2024, **14**, 28308

Metal-bipyridine supported on 3-aminopropyl-functionalized MK10: effect of a metalating agent on the catalytic activity in the transesterification of β-keto ester†

Adeyinka Sikiru Yusuff, *[ab] Yanlong Gu,[b] Elyor Berdimurodov[cd] and Ilyos Eliboev[ef]

The grafting of metal-bipyridine (Bpy-M, M = Mn or Zn) on aminopropyl-modified montmorillonite K10 (NH_2-MK10) synthesized *via* a functionalization-immobilization-metalation route was investigated. Formulated NH_2-MK10-Bpy-Mn and NH_2-MK10-Bpy-Zn were characterized using BET, FTIR, SEM, XRD, CHNS and NH_3-TPD techniques and tested for the synthesis of butyl acetoacetate (BAT) *via* the transesterification of β-keto ethyl acetoacetate (EAA) with butanol (BTL). The influence of reaction parameters on the BAT yield was investigated using the Taguchi optimization approach. According to characterization data, the samples were mesoporous materials with a considerable number of acidic sites and diverse inorganic and organic functional groups, making them inorganic–organic hybrid catalysts. Optimization results showed that catalyst loading had the most significant impact on the BAT yield, followed by the BTL : EAA molar ratio and temperature, whereas the conversion time had the least impact on the reaction process. NH_2-MK10-Bpy-Mn outperformed NH_2-MK10-Bpy-Zn in the transesterification of β-keto EAA, achieving 96.1 ± 0.79% conversion compared to 87.3 ± 0.94% at 110 °C for 7 h with a BTL : EAA molar ratio of 1.4 : 1 and catalyst loading of 2.0 wt%. Both catalysts were reusable and maintained good stability, which indicate their great potential for catalyzing the transesterification of β-keto ester.

Received 4th July 2024
Accepted 4th August 2024

DOI: 10.1039/d4ra04834b

rsc.li/rsc-advances

1. Introduction

With the introduction of green technology/chemistry, there has been growing pressure on chemical industries to develop processes that are environmentally friendly.[1] On this basis, the exploitation of merits of both homogeneous and heterogeneous catalysts has gained much interest recently as they help in upholding the main principles of green chemistry. The subject of fine chemicals and developing appropriate technology for their industrial synthesis have recently dominated the global scene. In this case, the transesterification of β-keto esters to produce acetoacetate (ester) compounds is an important organic fine chemical synthesis route, which requires suitable catalysts and favourable reaction conditions. β-Keto esters are compounds with both nucleophilic and electrophilic sites and are useful in pharmaceutical industry as they are the main building blocks of complex medicinal compounds such as prunustatin and (.+-.)-velloziolone.[2,3]

Generally, the production of esters *via* the transesterification process requires acidic or basic conditions and the utilization of one of the reactants in excess to enhance the target product yield.[4] According to Hennessy and Sullivan,[3] the transesterification kinetics of β-keto esters is greatly slow, and therefore, a catalyst is needed to create more molecular pathways for the reaction to improve the rate of the reaction. Some catalysts that have been used for the conversion of β-keto esters *via* the transesterification approach include traditional homogeneous catalysts (HCl, H_2SO_4, and *p*-TSA),[1] soluble basic and acidic catalysts (metal alkoxides, carbonates, metal chlorides, 4-dimethylaminopyridine, sodium perborate, zinc iodide, distannoxane, *etc.*),[5–9] heterogeneous acids and bases (Mo–ZrO_2, Y_2O_3–ZrO_2, Nb_2O_5, zinc dust, Amberlyst-15, sulfonated-SnO, NDEAP-SiO_2, Ag–Cu/hydrotalcite, *etc.*)[4,10,11] and functionalized

[a]*Department of Chemical and Petroleum Engineering, College of Engineering, Afe Babalola University, Km 8.5, Afe Babalola Way, Ado-Ekiti, Ekiti State, Nigeria. E-mail: yusuffas@abuad.edu.ng*

[b]*Institute of Physical Chemistry and Industrial Catalysis, School of Chemistry and Chemical Engineering, Huazhong University of Science and Technology, 1037 Luoyu Road, Hongshan District, Wuhan 430074, China*

[c]*Department of Chemical and Material Engineering, New Uzbekistan University, 54 Mustaqillik Avenue, Tashkent, 100007, Uzbekistan*

[d]*Department of Physical Chemistry, National University of Uzbekistan, Tashkent, 100034, Uzbekistan*

[e]*Uzbek-Finnish Pedagogical Institute, Spitamen Street, 166-home, Samarqand, Uzbekistan*

[f]*Department of Physics and Chemistry, Western Caspian University, A-Z-1001, Baku, Azerbaijan*

† Electronic supplementary information (ESI) available. See DOI: https://doi.org/10.1039/d4ra04834b

mesoporous materials (carbon nitride, MK10, nitrogen-ordered mesoporous carbon, H-β zeolite, mpg-C_3N_4, *etc.*).[12–16] Recently, a comprehensive list of different catalysts for the transesterification of β-keto esters has been compiled by Hennessy and Sullivan.[3]

The use of heterogenized homogeneous catalysts, particularly reusable inorganic–organic hybrid metal-based catalysts, in the transesterification of β-keto esters with alcohol and solvent was first reported by Sharma and Rawat.[1] To the best of our knowledge and based on literature reports, since then no similar studies have been reported, and thus it is timely to carry out a new study on the transesterification of β-keto esters using an efficient and reusable heterogenized homogeneous catalyst. In the work reported by Sharma and Rawat,[1] a silica-based inorganic–organic zinc catalyst was used to catalyze the transesterification of β-keto esters with different alcohols in toluene under the similar conditions, and the catalyst exhibited good stability after being reused nine times. However, the use of functionalized MK10 as a support to heterogenize zinc and manganese chlorides and as catalysts for the transesterification of β-keto esters have never been considered. Moreover, the optimization of the reaction parameters affecting the transesterification of β-keto esters using the experimental design methodology has never been reported to date. The favourable attributes of MK10, such as high silica content, large surface area, thermal and mechanical stability and ion-exchange capacity have attracted attention for further investigation.[17,18] Clay is a naturally innocuous material. Thus, the utilization of clay as a catalyst for chemical reactions is a promising aspect of green chemistry. Furthermore, clay is affordable, nontoxic, chemically diverse, and recyclable, making it appropriate for the commercial production of naturally occurring physiologically active chemicals.[18,19] The form of clay material used in this investigation can be found locally. To modify the surface of commercial MK10 with various activating agents, MK10 was used as a model catalyst during the conversion of β-keto ester (ethyl acetoacetate, EAA) to butyl acetoacetate (BAT). However, it has been reported that unmodified MK10 exhibits low catalytic activity in the transesterification of β-keto esters.[6] Therefore, the enhancement of MK10 through functionalization, immobilization and metallation is important to enhance its acidic attributes and activity. It should be noted that 3-aminopropyl triethoxysilane (TESPA) and di(2-pyridyl) ketone were chosen as modifying agents for this study based on their stability with a wide variety of structured supports, the presence of hydrogen bond forming functional groups, their commercial availability and eco-friendliness.

Another aspect of the transesterification of β-keto esters that needs much attention is the quest for favourable reaction conditions. Most of the previous studies focused on the synthesis of catalysts and their behaviour in the transesterification process.[1,20] Alternatively, studies on the impact of the parameters influencing the transesterification process using an optimization tool have never been reported to date. Therefore, it is timely to carry out optimization studies on the transesterification of β-keto esters over solid catalysts. To optimize the effective parameters with the minimum number of experiments, the application of experimental design methodologies (EDMs) can be useful. The Taguchi optimization approach is one of the EDMs used to control a process and optimize the process procedures to determine the favourable optimum conditions.[21] However, there is lack of information on the optimization of EAA conversion to BAT over inorganic–organic hybrid catalysts using the Taguchi experimental design approach.

Simple β-keto esters, such as EAA, are used to produce BAT because of their wide use as chemical intermediates in the synthesis of a wide variety of compounds. Therefore, the present study focused on the conversion of EAA to BAT *via* the transesterification process with MK10-based inorganic–organic hybrid zinc and manganese catalysts. The catalysts were prepared *via* the impregnation of metal chlorides of zinc and manganese on functionalized MK10 (see Scheme 1) and characterized using various analytical techniques (XRD, FTIR, SEM, NH_3-TPD, CHNS and BET) to gain insight into their properties. The impact of the transesterification process parameters (temperature, catalyst dosage, time and alcohol/EAA molar ratio) was studied using the Taguchi approach. Moreover, the reusability of the catalysts was investigated to examine their stability during reuse.

2. Materials and methods

2.1. Materials

All the laboratory-grade reagents, including montmorillonite K10 (MK10, Alfa Aesar), butanol (BTL, 99.5%, Sigma-Aldrich), EAA (99%, Energy Chemical), di(2-pyridyl) ketone (98%, Merck), zinc chloride ($ZnCl_2$), manganese chloride ($MnCl_2$), anhydrous ethanol (99.5%, Merck), anhydrous toluene (99.8%, Merck), *n*-hexane (99%, Sigma-Aldrich), ethyl acetate (99.9%, Merck) and 3-aminopropyl triethoxysilane (TESPA, 98%, Energy Chemical), were purchased from Chemical Stores in Wuhan, China and utilized as received.

2.2. Catalyst synthesis

2.2.1. Preparation of aminopropyl-modified MK10 (NH_2-MK10). The functionalization of MK10 was carried out by adopting the procedures reported by Sharma and Rawat.[1] Typically, 15 mL of TESPA was added to 5 g of MK10 suspended in 10 mL distilled water under constant stirring at 50 °C for 1 h. Subsequently, the resultant mixture was filtered, and the obtained residue was washed with distilled water until its pH attained 6.0, and then dried at 80 °C overnight to obtain aminopropyl-modified MK10, which is henceforth called NH_2-MK10.

2.2.2. Formulation of surface-bound chelating ligand (NH_2-MK10-Bpy). In this case, 6.0 g of NH_2-MK10 was refluxed with di(2-pyridyl) ketone (3 mmol, 0.552 g) in 50 mL anhydrous toluene at 80 °C for 12 h. Thereafter, the mixture was filtered and the obtained residue was thoroughly washed with warm toluene five times to get rid of the unbound ligands. Subsequently, the solid was dried for 11 h at 100 °C to obtain NH_2-MK10-Bpy.

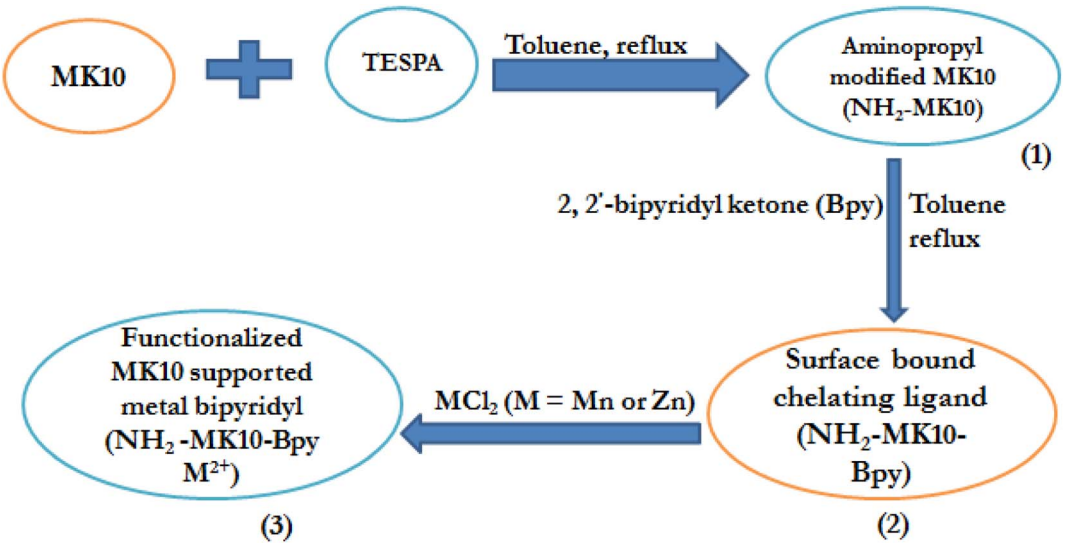

Scheme 1 Synthesis of the montmorillonite K10 (MK10)-based metal-bipyridyl catalyst.

2.2.3. Synthesis of functionalized MK10 supported zinc- and manganese-bipyridyl (NH_2-MK10-Bpy-Zn and NH_2-MK10-Bpy-Mn). The NH_2-MK10-Bpy-M^{2+} catalysts were prepared *via* a modified procedure, as reported by Sharma and Rawat.[1] The $ZnCl_2$ and $MnCl_2$ suspensions were prepared by dissolving $ZnCl_2$ (0.5 g, 3.7 mmol) and $MnCl_2$ (0.5 g, 4.0 mmol) in 50 mL of anhydrous ethanol in different containers, and thereafter 5.0 g of NH_2-MK10-Bpy was added to each suspension and stirred overnight at ambient temperature. The solvent was decanted and the wet catalyst was thoroughly washed in 50 mL of ethanol. Subsequently, the washed solid sample was oven-dried at 100 °C for 2.5 h to obtain the NH_2-MK10-Bpy-Zn and NH_2-MK10-Bpy-Mn catalysts.

2.3. Analysis of formulated solid materials

The crystallographic framework of MK10 was evaluated by XRD analysis using a Bruker D8 Advance X-ray diffractometer. Cu-kα radiation (λ = 1.542 Å) was employed to generate the XRD profile in the 2θ range of 5° to 80° at a scanning rate of 2° min^{-1}. The textural properties (pore volume, pore diameter and specific surface area) of the formulated samples were determined on a Micromeritics porosity analyzer (ASAP2460, USA) with N_2 gas (as adsorbate) at −196 °C. Each sample was degassed at 230 °C for 5 h to get rid of adsorbed gases and moisture from their surface. The infrared spectra of the prepared samples were recorded in the range of 4000–400 cm^{-1} on a ThermoFisher-Scientific FTIR spectrophotometer. The FTIR analysis provided information regarding the functional groups present on the surface of the samples. The morphological attributes of the solid materials were examined under a Sigma-300 scanning electron microscope, while the acid strengths of the solid acid catalysts were measured by temperature-programmed desorption-NH_3 analysis using a Japan Bayer BELCAT-A TPD/TPR/TRO analyzer. Furthermore, the compositions of atomic carbon, hydrogen, nitrogen and sulfur were determined using a CHNS analyzer. Additionally, the total acid densities of the as-prepared catalyst were determined *via* the titration method reported in our previous study.[22] Briefly, 0.1 g of solid material was suspended in 25 mL of NaCl solution (2.0 M) and stirred on a magnetic stirrer for 20 min to allow ion exchange between the solid acid catalyst and sodium salt. Thereafter, the stirred suspension was filtered, and the filtrate was titrated against 0.05 M NaOH using phenolphthalein as the indicator. The total acid density (A_T) of the catalyst was estimated using eqn (1), as follows:

$$A_T = \frac{V_{NaOH} \times C_{NaOH}}{W_C} \quad (1)$$

where V_{NaOH} = volume of NaOH consumed, C_{NaOH} = concentration of NaOH consumed and W_C = weight of catalyst sample used.

2.4. Catalytic activity evaluation during transesterification of EAA with BTL

The transesterification of EAA with butanol was carried out in a 50 mL round-bottom flask attached with a reflux condenser and a magnetic stirrer. For each reaction, the flask was immersed in a silicone oil bath to control the reaction temperature (Scheme 2). Typically, EAA (10 mmol, 1.30 g), BTL (15 mmol, 1.11 g), catalyst (0.04 g) and toluene (10 mL) were fed into the flask and continuous mixing began immediately after coupling of the reflux apparatus to ensure adequate contact between the reactants and catalyst. During the preliminary studies, the transesterification reaction was conducted at 110 °C for 6 h with a 1.5 : 1 molar ratio of BTL : EAA and 0.04 g catalyst (corresponding to 3.0 wt% of ethyl acetoacetate used).

The progress of the reaction was monitored by thin layer chromatography (TLC) using a mixture of *n*-hexane and ethyl acetate as the eluting solvent at a ratio of 9 : 1. At the end of the reaction, the mixture was left to cool and the catalyst was separated through centrifugation. The catalyst was regenerated by washing with 30 mL of *n*-hexane five times to remove

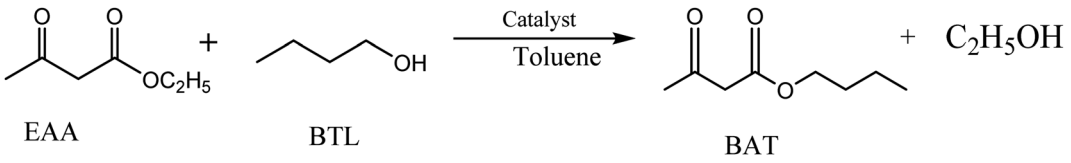

Scheme 2 Transesterification of EAA with BTL catalyzed by inorganic–organic hybrid catalysts.

physisorbed molecules and dried at 90 °C for 12 h. The supernatant was purified using a preparative TLC plate and a mixture of *n*-hexane and ethyl acetate (ratio 30 : 1) as the eluting solvent to isolate the desired product and the yield of the product was calculated as follows:

$$Y_I = \frac{W_p}{W_{EAA}} \times 100\%$$

where Y_I = isolated yield (%), W_p = weight of isolated product and W_{EAA} = weight of ethyl acetoacetate used.

2.4.1. Analysis of transesterification product. The product (butyl acetoacetate, BAT) produced during the transesterification reaction was analyzed to examine its chemical structure and purity *via* ^{1}H and ^{13}C-NMR spectroscopy with Bruker Avance III™ 500 MHz spectrometer using deuterated chloroform ($CDCl_3$) as the solvent. The obtained NMR data were calibrated and analyzed by using the MestReNova-14.12-25024 software.

2.5. Optimization of transesterification of EAA using the most active catalyst

To model and optimize the transesterification of β-keto ester with butanol over the most active catalyst, four independent factors were considered at the four factor-three level L_9 orthogonal of the Taguchi design approach. The level selection was done based on the preliminary experiments conducted and literature reports. The established limits were incorporated in the Design-Expert software (Version 12, Stat Ease), which suggested 9 transesterification reaction runs, as illustrated in Table 1. The isolated yield (%) of the desired product was considered as the process output, while temperature, *T* (°C), catalyst quantity, *C* (wt%), molar ratio of BTL : EAA, *M* and reaction time, *t* (h) were independent process parameters.

Furthermore, the signal/noise (S/N) ratio, which is a logarithmic parameter used to compare the response to the desired value, was estimated based on values of product yields obtained.[21] The S/N ratio can be group into three categories, namely nominal is better (NB), smaller is better (SB) and larger is better (LB). The experimental values obtained from the transesterification of EAA with BTL were analyzed using the LB criterion (eqn (2)) to evaluate the optimum process variables and study the contribution of each parameter that influences the β-keto ester conversion process.

$$(S/N)_{LB} = -10 \log\left[\frac{1}{n}\sum_{i=1}^{n}\frac{1}{y_i^2}\right] \quad (2)$$

where y_i and n are the measured response and number of repetitions under similar experimental conditions, respectively.

Table 1 Studied reaction process parameters and their associated levels

		Levels		
Factors	Description	L1	L2	L3
T	Temperature (°C)	100	110	120
C	Catalyst amount (wt%)	1.0	2.0	3.0
M	BTL : EAA molar ratio	1.3 : 1	1.4 : 1	1.5 : 1
T	Time (h)	5.0	6.0	7.0

3. Results and discussion

3.1. Catalysts characterization

Several characterization approaches, including XRD, FTIR, SEM, NH_3-TPD, CHNS and BET, were used to evaluate the physicochemical properties of the synthesized solid materials and the analysis results are discussed as follows.

The X-ray diffractogram of the MK10 sample is displayed in Fig. 1 with numerous high intense peaks, corresponding to the SiO_2 (20.13°, 25.86°, 26.9°, 39.68° and 68.1°), Al_2O_3 (18.06°, 35.24° and 54.69°), and Ca_2AlSiO_2 (42.36°) phases. The presence of peaks associated with both SiO_2 and Al_2O_3 suggests that the MK10 sample is an aluminosilicate material and can serve as a good structured support for the synthesis of heterogenized homogeneous catalysts. This was corroborated by the results of the textural properties analysis, in which the surface area, pore volume and pore diameter of the prepared solid materials were evaluated. The textural properties of MK10, NH_2-MK10, NH_2-

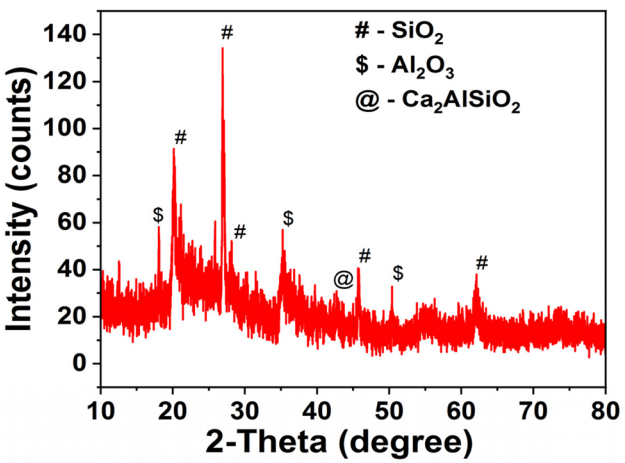

Fig. 1 XRD pattern of the MK10 sample.

MK10-Bpy, NH_2-MK10-Bpy-Zn and NH_2-MK10-Bpy-Mn are presented in Table 2. As depicted by the results, the surface area and average pore volume of MK10 were 228.1 $m^2\ g^{-1}$ and 0.381 $cm^3\ g^{-1}$, respectively, which decreased upon its modification with aminopropylating reagent, suggesting the dispersion of TESPA on the structured support. It is worth noting that the surface area and pore volume were less pronounced after the impregnation of di(2-pyridy) ketone and metallation with Zn and Mn chlorides. The pore diameter of MK10 was found to be smaller than that of the other materials, suggesting the possible inclusion of mesopores in the catalyst support, which in turn reduced the surface area and pore volume.[18] The mesoporous nature of the catalytic materials enhanced their performance in the transesterification reaction because a large pore diameter can promote the rapid adsorption of the reactant onto the surface of the catalyst, which facilitates the reaction process. Similarly, a slight decrease in the surface area was reported during the preparation of the silica gel-based zinc bipyridyl (SG-NH_2-Bpy-Zn) catalyst, as reported by Sharma and Rawat.[1] The possibility of the formation of a metal multilayer on the ligand-grafted MK10 surface during metallation could not be ignored. This observation agreed with the view by Amani *et al.*[23] who reported that the multilayer dispersion of metals reduces the surface area and causes the partial blockage of pores. Nevertheless, the blockage of the catalyst pores does not represent low activity given that there were active acidic sites on the formulated catalysts. This was corroborated by the NH_3-TPD profiles of MK10, NH_2-MK10-Bpy-Zn and NH_2-MK10-Bpy-Mn, as display in Fig. 2. As seen from the results, MK10 exhibited a single desorption peak at 129 °C, which can be ascribed to the interaction of NH_3 with the weak acidic sites.[24] According to Nda Umar *et al.*,[25] the desorption peaks between <100 °C and 200 °C are associated with sites of the weak acidic strength, and also suggest the presence of oxygen-containing functional groups on the material surface. The total acid site (acidity) of the MK10 sample was 37 μmol NH_3/g, which suggested a low acidic strength. However, both NH_2-MK10-Bpy-Zn and NH_2-MK10-Bpy-Mn displayed more than one NH_3 desorption peak. The NH_3-TPD profile of NH_2-MK10-Bpy-Zn exhibited three peaks at 112 °C (weak acidic site), 335 °C (medium to strong acidic site) and 388 °C (medium to strong acidic site), while that of NH_2-MK10-Bpy-Mn displayed four desorption peaks at 114 °C (weak acidic site), 279 °C (medium to strong acidic site), 405 °C (strong acidic site) and 478 °C (strong acidic site). These results suggested the improvement in acidity due to functionalization,

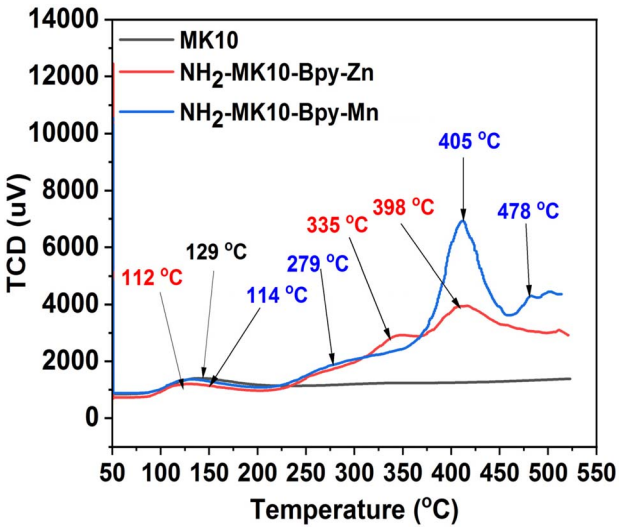

Fig. 2 NH_3-TPD profiles of MK10, NH_2-MK10-Bpy-Zn and NH_2-MK10-Bpy-Mn.

immobilization and metallation effects. The total acid sites in NH_2-MK10-Bpy-Zn and NH_2-MK10-Bpy-Mn were estimated to be 439 and 563 μmol NH_3/g, respectively. The strong acidic strength of NH_2-MK10-Bpy-Mn was attributed to the fact that the NH_3 desorption peak appeared at a higher temperature and the high intensity peak suggested that this catalyst has a larger acidic concentration compared to NH_2-MK10-Bpy-Zn, making the former more denser in terms of total acid sites and accessible by the substrate, consequently enhancing the reaction product yield.[26] The total acid density for the MK10, NH_2-MK10-Bpy-Zn and NH_2-MK10-Bpy-Mn samples was determined *via* the titration method to be 0.05 ± 0.010, 1.94 ± 0.34 and 2.79 ± 0.08 mmol g^{-1}, respectively, which is consistent with the results of the NH_3-TPD analysis. These observations indicated that the interaction between the metal (Zn, Mn) chlorides and ligand-grafted MK10 (NH_2-MK10-Bpy) resulted in the formation of catalysts (NH_2-MK10-Bpy-Zn and NH_2-MK10-Bpy-Mn) with a significant number of acidic sites, which were responsible for the high catalytic activities during the transesterification of EAA.

The obtained results from the FTIR analysis are displayed in Fig. 3, where the spectra of all the analyzed samples exhibited broad bands at around 3600–3500 cm^{-1}, revealing the presence of adsorbed moisture and O–H stretching, and these bands were ascribed to the stretching modes of internal and external

Table 2 Physicochemical properties of MK10 and modified MK10 samples

	Ultimate analysis[a] (%)				Textural properties		
Sample	C	H	N	C/N	Surface area ($m^2\ g^{-1}$)	Pore volume ($cm^3\ g^{-1}$)	Average pore diameter (Å)
MK10	—	—	—	—	228.1	0.381	6.39
NH_2-MK10	3.84	1.72	4.0	0.96	164.3	0.295	14.32
NH_2-MK10-Bpy	12.38	2.03	6.05	2.05	143.6	0.271	38.53
NH_2-MK10-Bpy-Zn	11.51	2.28	5.71	2.02	101.8	0.257	21.82
NH_2-MK10-Bpy-Mn	10.90	2.11	5.70	1.91	106.2	0.318	27.09

[a] Evaluated by CHNS analyzer.

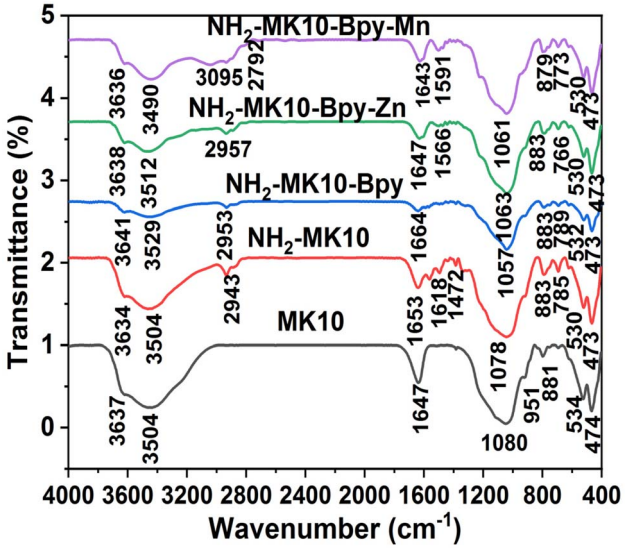

Fig. 3 FTIR spectra of MK10, NH_2-MK10, NH_2-MK10-Bpy, NH_2-MK10-Bpy-Zn and NH_2-MK10-Bpy-Mn.

hydroxyl functional groups, similar to that reported elsewhere.[18] A band at around 2950 cm^{-1}, which is attributed to the C–H stretching of the methyl group, was observed in the spectra of NH_2-MK10, NH_2-MK10-Bpy-Zn and NH_2-MK10-Bpy-Mn as a consequence of MK10 functionalization with TESPA, and also indicated that the amine groups were anchored on the MK10 surface,[27] as corroborated by the CHN results (see Table 2), in which the N element was found in the samples. The transmittance pattern in the FTIR analysis revealed the presence of Si–O–M^+ deformation, NH stretching in the secondary amides, in-plane-OH bending due to carboxylic acid, O–Si–O stretching and M^+–OH bending at around 1650–1620 cm^{-1}, 1560–1590 cm^{-1}, 1472 cm^{-1}, 1100–1000 cm^{-1} and 951 cm^{-1}, respectively, which are consistent with studies reported elsewhere.[18] According to similar findings reported by Sharma and Rawat,[1] the peak at around 1640 cm^{-1} indicated the formation of imine, suggesting the anchoring of bipyridyl ketone on the surface of the functionalized MK10. It is worth noting that all the samples exhibited a sharp and strong peak at around 1100 cm^{-1}, which confirmed the presence of silanol functional groups and suggested a material with a high silica content.[28,29] However, the absorption bands observed in the spectra of all the analyzed samples below 1000 cm^{-1} correspond to metal–oxygen bonds, similar to the studies reported elsewhere.[30,31] These bands can also be attributed to the asymmetric and symmetric stretching of the silaxane group ν(Si–O–Si).[1] Therefore, according to the FTIR data, it was possible to elucidate the bonding interaction and typical spectra of MK10 and the modifying agents.

The external morphological structures of the formulated solid materials are displayed in Fig. 4. MK10 exhibited a relatively rough surface with some flower-like shapes, and its particles were agglomerated into a larger mass, in excellent agreement with the results reported by Olutoye *et al.*[18] Some pores appeared on the surface of NH_2-MK10 and the particles were smaller compared to that of the untreated support sample, which is attributed to the functionalization effect. The size of the amine-functionalized MK10 particles was further reduced, the particles merged and their shapes become more irregular after the immobilization of bipyridyl ketone. These observations were due to the changes in the composition of MK10 as a consequence of its grafting with organic reagents. Fig. 4d and e show that the interaction between the metal chlorides and ligand-grafted MK10 (NH_2-MK10-Bpy) resulted in the formation of catalysts (NH_2-MK10-Bpy-Zn and NH_2-MK10-Bpy-Mn) with porous frameworks, which made them sufficiently active in the transesterification of EAA, respectively. The ultimate analysis results are displayed in Table 2 with the N contents in NH_2-MK10, NH_2-MK10-Bpy, NH_2-MK10-Bpy-Zn and NH_2-MK10-Bpy-Mn found to be 4.0%, 6.05%, 5.71% and 5.70%, respectively. In terms of C/N ratio, NH_2-MK10-Bpy, NH_2-MK10-Bpy-Zn and NH_2-MK10-Bpy-Mn exhibited higher ratios compared to NH_2-MK10, which confirmed the incorporation of TESPA and di(2-pyridyl) ketone in the MK10 matrix.

3.2. Isolated product yields of the catalytic samples

The catalytic activity of each of the formulated samples was investigated during the transesterification of EAA with BTL, and the corresponding isolated yields are listed in Table 3. The results revealed that no reaction occurred when the reaction was conducted without the catalyst (entry 1) and when it was catalyzed by the unmodified MK10 (entry 2). This observation indicated that the transesterification of EAA with BTL using toluene as the solvent was a catalyst-driven reaction. In addition, ineffectiveness of MK10 during the reaction signified that the acidic site of the support was not adequately active to drive the transesterification reaction to equilibrium. A reaction was noticed when NH_2-MK10 (entry 3) and NH_2-MK10-Bpy (entry 4) were used as catalysts, though the isolated yields were <30%, suggesting that the aminopropylation of MK10 and immobilization of bipyridyl ketone on NH_2-MK10 slightly improved the acidity of the resulting solid materials, respectively, as corroborated by the results from NH_3-TPD analysis (see Fig. 2). However, the isolated yield significantly increased upon metallation of NH_2-MK10-Bpy with $ZnCl_2$ and $MnCl_2$, which is attributed to the increase in the number of acidic sites on the surface of the catalysts, acting as active centers during the transesterification reaction. It is worth noting that NH_2-MK10-Bpy-Mn performed better than NH_2-MK10-Bpy-Zn because the manganese-based catalyst has a unique ability to catalyze the transesterification reaction without altering the chemical stability of the keto carbonyl group of the β-keto ester, as reported by Li *et al.*[6] Moreover, using toluene as the solvent in the transesterification reaction catalyzed by the Mn-based catalyst inhibits occurrence of side reactions, which may be caused as a result of the reactivity of the keto carbonyl group in the β-keto ester under acidic conditions toward some nucleophiles.[32]

3.3. Optimization of transesterification of EAA using the most active catalyst

Table 4 shows the results obtained from the transesterification experiments, including the L_9 orthogonal design matrix, BAT yields and values of S/N ratio. As indicated by the results, different values of BAT yield were achieved at different

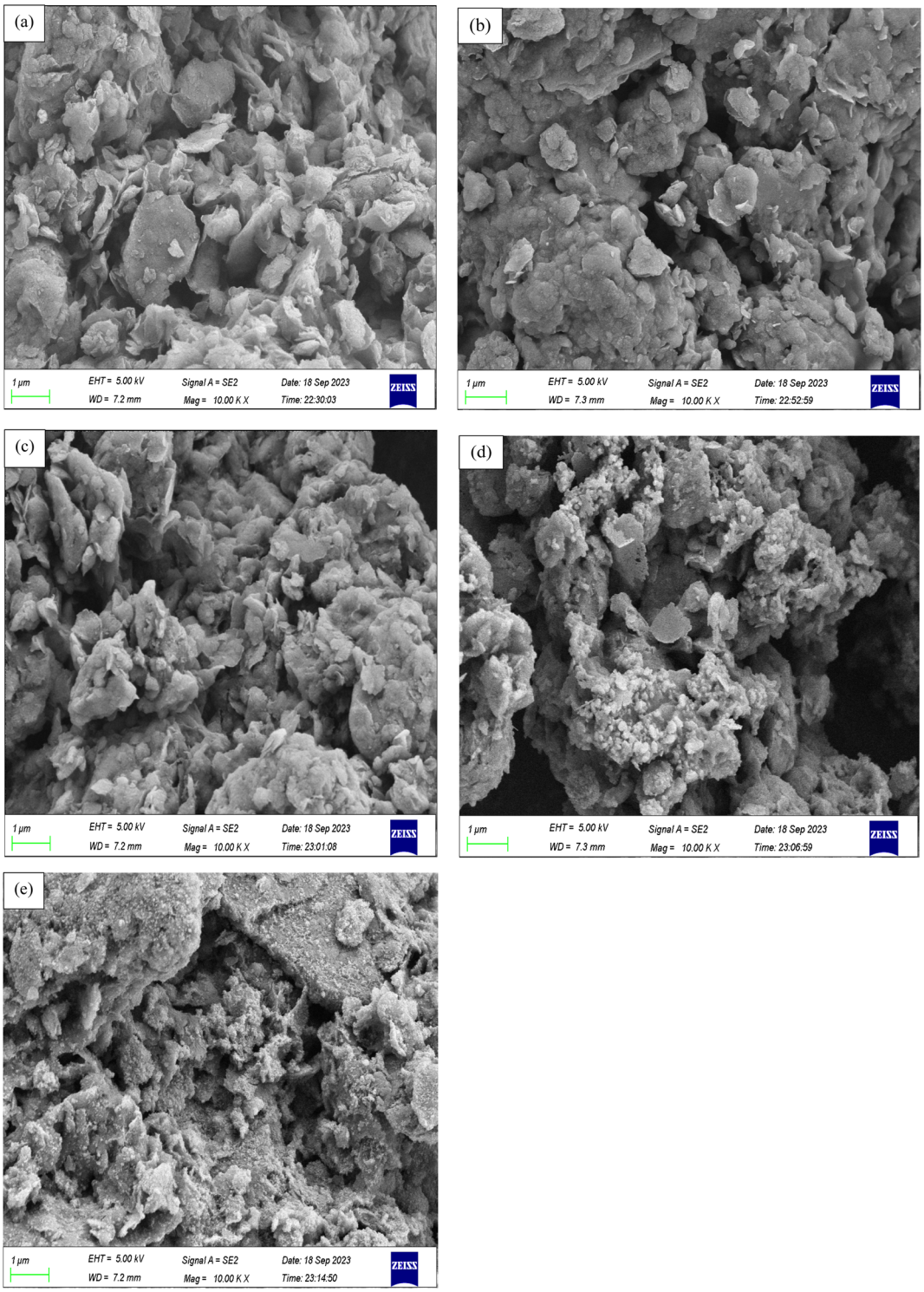

Fig. 4 SEM images of (a) MK10, (b) NH_2-MK10, (c) NH_2-MK10-Bpy, (d) NH_2-MK10-Bpy-Zn and (e) NH_2-MK10-Bpy-Mn.

operating conditions with run 5 offering the highest BAT yield (95.4%) at 100 °C for 6.0 h with a BTL : EAA molar ratio of 1.4 : 1 and 2.0 wt% NH_2-MK10-Bpy-Mn amount.

Additionally, the combined plot of S/N ratio against the transesterification process conditions, which was used to determine the optimum values of the parameters involved, is shown in Fig. 5. As evidenced by the obtained results, the maximum BAT yield was achieved at the middle level of temperature (110 °C). A higher temperature promotes the diffusion of reactants and dispersion of the solid catalyst particles. Although high temperature promotes the catalyst–reactant–solvent interaction and ion transfer, which will result in a high EAA conversion, a reaction temperature above the boiling point (117.7 °C) of butanol may lead to its vaporization,

Table 3 Transesterification of EAA with BTL using different catalysts[a]

Entry	Catalyst	Reaction time (h)	Yield (%)
1	Blank	6.0	NR
2	MK10	6.0	NR
3	NH_2-MK10	6.0	6.3 ± 0.02
4	NH_2-MK10-Bpy	6.0	21.7 ± 0.31
5	$ZnCl_2$	6.0	56.5 ± 0.03
6	$MnCl_2$	6.0	61.3 ± 0.46
7	NH_2-MK10-Bpy-Zn	6.0	81.3 ± 0.20
8	NH_2-MK10-Bpy-Mn	6.0	93.4 ± 0.77

[a] Reaction conditions: EAA (10.0 mmol), BTL (15.0 mmol) and catalyst (0.04 g) in toluene (10 mL) was refluxed at 110 °C for 6.0 h. NR: no reaction.

and consequently reduce the product yield.[33] As displayed in Fig. 5b, the BAT yield increased with an increase in the content of NH_2-MK10-Bpy-Mn, and then decreased as the catalyst amount increased above 2.0 wt%. This finding suggests that 2.0 wt% catalyst concentration was adequate to shift the transesterification reaction forward. Furthermore, the highest BAT yield was obtained at the middle level of BTL : EAA molar ratio (1.4 : 1 mol mol^{-1}), as evidenced in Fig. 5c. This observation suggests that the molar ratio of BTL to EAA at 1.4 : 1 is capable of shifting the reversible equilibrium to the forward direction and achieving the maximum product yield. It was noticed that the BAT yield decreased as the molar ratio increased above 1.4 : 1 because excess butanol inhibits the separation of the desired product from reaction mixture, which results in the final yield of the product.[34] According to the illustrated result in Fig. 5d, the BAT yield increased by increasing the transesterification duration, indicating that a longer reaction time facilitates stronger interaction between the reactant and catalyst, which leads to more frequent collisions, consequently promoting the conversion of ethyl acetoacetate. Some researchers reported that a sufficient reaction time is critical in achieving a high yield during the transesterification reaction.[31,35] Therefore, as displayed in Fig. 5, the optimal conditions for EAA conversion *via* transesterification were 110 °C, 2.0 wt%, 1.4 : 1 and 7 h for temperature, catalyst amount, BTL : EAA molar ratio and time, respectively. Under these conditions, the predicted BAT yield was 96.6% (S/N ratio = 39.7). Further transesterification experiments were conducted to validate the predicted dependent parameter, and the average observed BAT yield was found to be 96.1 ± 0.79% with the corresponding S/N ratio estimated to be 39.6.

3.3.1. Analysis of variance (ANOVA) for transesterification of EAA over NH_2-MK10-Bpy-Mn catalyst. ANOVA was employed to evaluate the significance of each of the heterogeneously catalyzed transesterification process parameters, and the obtained results are illustrated in Table 5. The results displayed some parameters, including probability of occurrence (*p*-value), Fisher's test (*F*-value) and contribution factor (CF, estimated by eqn (3)), which were used to examine the significance and contribution of each of the parameters. Additionally, the coefficient of determination (R^2), adjusted R^2 and predicted R^2 were used to further justify the significance of the model. The model parameter with a *p*-value of less than 0.05 and larger *F*-value and CF has significant influence on the process output.[36] However, in this study the results, as shown in Table 5, indicated that the catalyst amount had the most significant influence on the transesterification process, followed by the BTL : EAA molar ratio and reaction temperature. However, the reaction time had the least impact on the synthesis of butyl acetoacetate from EAA. Moreover, the R^2 value of 0.9888 indicated that 98.88% of the total variation was described by the operating variables studied, and it also implied that only 1.12% of the variation was not explained by the model. In addition, the predicted R^2 (0.9324) agreed reasonably well with the adjusted R^2 (0.9552), which signified the predictability of the model. Adeq precision evaluates the signal to noise ratio, where a value greater than 4 is desirable. However, in this study, the value of 13.51 suggests an adequate signal. Furthermore, the rank of the parameters, which is the range of S/N ratios for a particular parameter, was evaluated to corroborate the earlier findings, and the obtained results (see Table 6) confirmed that the catalyst amount (with 1st rank) had the most significant impact on BAT yield, followed by BTL : EAA molar ratio and temperature, while the transesterification time had the least impact on the heterogeneously catalyzed transesterification reaction.

$$\mathrm{CF} = \left[\frac{SS_i}{\sum SS_i}\right] \times 100\% (i \neq 0) \quad (3)$$

where SS_i and $\sum SS_i$ are the sum of the square of a certain parameter and total sum of the square of all the parameters.

Table 4 L_9 orthogonal array design, BAT yields and S/N ratios

	Transesterification process factors				Butyl acetoacetate, BAT yield	
Run no.	Temperature, *T* (°C)	Catalyst amount, *C* (wt%)	BTL : EAA molar ratio, *M*	Time (h)	Experimental value (%)	S/N ratio
1	120	1.0	1.5 : 1	6.0	51.3 ± 1.04	34.2
2	100	1.0	1.3 : 1	5.0	45.9 ± 0.34	33.2
3	110	2.0	1.5 : 1	5.0	87.4 ± 0.01	38.8
4	100	3.0	1.5 : 1	7.0	68.1 ± 0.84	36.7
5	100	2.0	1.4 : 1	6.0	95.4 ± 0.31	39.6
6	110	3.0	1.3 : 1	6.0	89.3 ± 0.56	39.1
7	120	3.0	1.4 : 1	5.0	92.7 ± 2.51	39.3
8	110	1.0	1.4 : 1	7.0	79.5 ± 0.96	38.0
9	120	2.0	1.3 : 1	7.0	91.4 ± 0.47	39.2

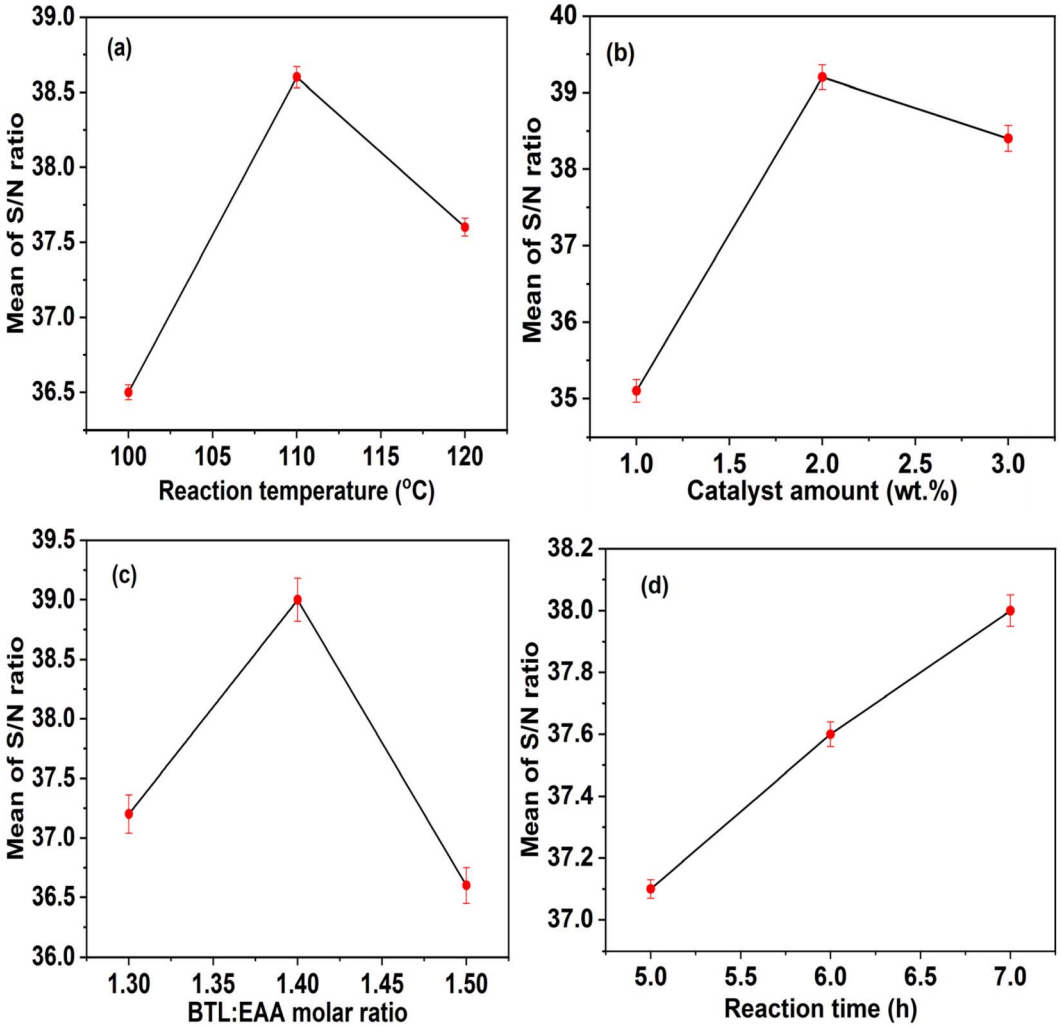

Fig. 5 Plots of mean of the S/N ratio as a function of (a) temperature, (b) catalyst amount, (c) the BTL : EAA molar ratio and (d) reaction time.

3.4. Comparison between NH_2-MK10-Bpy-Zn and NH_2-MK10-Bpy-Mn and other solid catalysts for the transesterification of EAA

To compare the catalytic performance of NH_2-MK10-Bpy-Zn and NH_2-MK10-Bpy-Mn under the optimum operational conditions (temperature = 110 °C, catalyst amount = 2.0 wt%, conversion time = 7 h and BTL : EAA molar ratio of 1.4 : 1) previously obtained (see Section 3.3), NH_2-MK10-Bpy-Zn was used to catalyze the transesterification reaction under these conditions. The BAT yields of 96.1 ± 0.79% and 87.3 ± 0.94% were obtained for NH_2-MK10-Bpy-Mn and NH_2-MK10-Bpy-Zn, respectively. Thus, NH_2-MK10-Bpy-Mn exhibited the best catalytic performance as a consequence of its large surface area and significant number of active sites, which enhanced the EAA conversion to

Table 5 ANOVA results for the BAT yield

Source	Sum of squares	df	Mean square	*F*-value	*p*-value	% Contribution
Model	2727.02	6	454.50	29.43	0.0332 significant	
T	366.54	2	183.27	11.87	0.0777	13.4%
C	1719.40	2	859.70	55.66	0.0176	63.1%
M	641.08	2	320.54	20.75	0.0460	23.5%
Residual	30.89	2	15.44			
Cor. total	2757.91	8				
R^2	0.9888					
Adjusted R^2	0.9552					
Predicted R^2	0.9324					
Adeq. precision	13.51					

Table 6 Response data of average S/N ratios for BAT production conditions

Level	Temperature (°C)	Catalyst amount (wt%)	BTL : EAA molar ratio	Time (h)
1	36.5	35.1	37.2	37.1
2	38.6	39.2	39.0	37.6
3	37.6	38.4	36.6	38.0
Range	2.1	4.1	2.4	0.9
Rank	3rd	1st	2nd	4th

BAT. It is worth noting that the BAT yield obtained in this study was higher than the yield reported by Sharma and Rawat.[1] In their work, the BAT yield of 92% was obtained at 120 °C for 4 h with a BTL : EAA molar ratio of 1.2 : 1 and catalyst (SG-NH_2-Bpy-Zn) concentration of 2.0 wt%. Although different alcohols were used for the same reaction, our product yield was also higher than that reported by Sathicq *et al.*,[37] who carried out the transesterification of EAA with different alcohols in refluxing toluene over a heterogeneous catalyst (SAF) synthesized using modified silica and 3-aminopropyltriethoxysilane. The product yields of 92%, 92%, 95%, 52% and 77% were obtained when 3-phenyl-propanol, 4-methoxybenzyl alcohol, geraniol, linalool and menthol were used as alcohols, respectively.[37] In their work, the reaction times were between 4 and 14 h, whereas the transesterification of EAA with BTL conducted in the current study lasted for 7 h. This observation indicates that both the alcohol type and reaction time play crucial roles in the transesterification of β-keto esters.

3.5. Studies on NH_2-MK10-Bpy-Zn and NH_2-MK10-Bpy-Mn stability

The reusability of NH_2-MK10-Bpy-Zn and NH_2-MK10-Bpy-Mn were evaluated for five transesterification reaction cycles at 110 °C with a 1.4 : 1 BTL : EAA molar ratio and catalyst amount of 2.0 wt% for 7 h, and the results are illustrated in Fig. 6. The BAT yields were 83.1% and 52.7% in the first and fifth runs, when NH_2-MK10-Bpy-Mn was reused to catalyze the transesterification of EAA with BTL, while the yields in the first and fifth runs were 72.8% and 38.1% for NH_2-MK10-Bpy-Zn, respectively. The observed decrease in yield can be attributed to the obstruction of the catalyst pores/active sites by the reactant molecules. Furthermore, the loss of catalytic activity possibly occurred during the catalyst regeneration process, causing a reduction in the transesterification product yield. To verify this claim, a leaching test was carried out by mixing the fresh catalyst with BTL at 50 °C for 2 h. BTL was recovered *via* centrifugation and utilized for the transesterification of EAA at 110 °C for 7 h with the EAA to BTL molar ratio of 1.4 : 1 mol mol^{-1} and catalyst amount of 2.0 wt%. Moreover, a catalyst-free transesterification experiment was carried out with EAA and pure BTL in toluene under the same conditions. The alcoholysis of EAA with the used BTL in the absence of the catalyst resulted in <5% BAT yield, indicating the leaching of the catalyst active sites during the reaction. However, no reaction occurred when pure BTL was used without catalyst, which confirmed the leaching of the catalyst. Therefore, the observed decline in transesterification product yield during successive reaction cycles was attributed to the loss of the active centers during the reaction or catalyst recovery operation. This observation was also corroborated by the obtained values of total acid density for the two catalysts after 1st and 5th runs, which were determined to be 1.81 ± 2.04 and 0.54 ± 0.96 mmol g^{-1} for NH_2-MK10-Bpy-Mn and 1.34 ± 0.08 and 0.21 ± 0.08 for NH_2-MK10-Bpy-Zn, respectively. Nevertheless, both catalysts exhibit great potential to be employed to catalyze the conversion of β-keto esters given that they showed good stability and recyclability during the transesterification reaction.

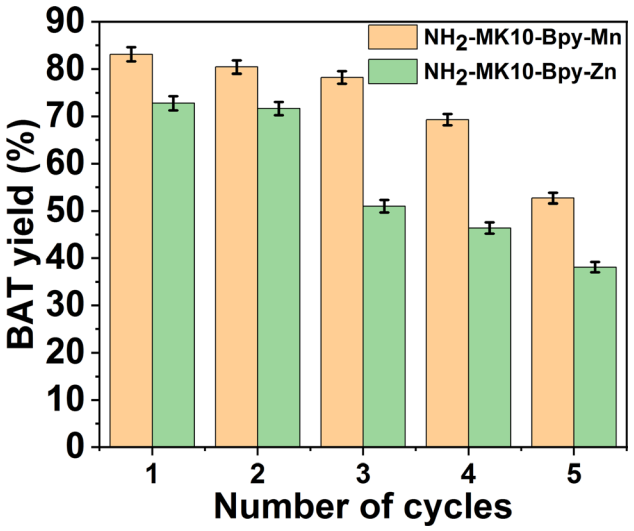

Fig. 6 Reusability of NH_2-MK10-Bpy-Zn and NH_2-MK10-Bpy-Mn catalysts in the transesterification of EAA under optimum conditions.

3.6. Analysis of transesterification product obtained under the optimum conditions

To ascertain the quality of the isolated product obtained after the transesterification of EAA with BTL under the optimal conditions, its composition was examined by ^{1}H NMR and ^{13}C NMR analyses. The results are illustrated in Fig. SM1.† Based on the ^{1}H NMR spectrum (Fig. SM1a†), the signal related to a proton associating with a carbon atom bearing the β-ketone ester (C═O) group appeared at the chemical shift of δ = 2.27 ppm, while the signal for the proton in the carboxylic acid (O–C═O) group was located at δ = 3.46 ppm. Furthermore, the signals for the protons associated with the hydrocarbon chain (butyl) appeared at δ = 0.93, 1.39, 1.63 and 4.15 ppm. In the case of the ^{13}C NMR spectrum shown in Fig. SM1b,† the carbons associated with the β-ketone ester (C═O) group appeared at δ = 50.03 ppm, while the signal related to a carbon for the carboxylic acid group was noticed at δ = 65.15 ppm. In addition, the signal for carbon directly attached to the ester group was noticed at δ = 30.03 ppm. These findings revealed that the signal responses for the obtained product corresponded to the butyl (C_4H_9) structure and ester ($C_4H_5O_3$) group and are in excellent agreement with the results reported elsewhere,[38]

suggesting that the synthesized product is the target butyl acetoacetate.

4. Conclusions

Herein, the formulation and analysis of novel NH_2-MK10-Bpy-M^+ hybrid catalysts were successfully carried out. The metallation of NH_2-MK10-Bpy with $ZnCl_2$ and $MnCl_2$ resulted in NH_2-MK10-Bpy-Zn and NH_2-MK10-Bpy-Mn, respectively. The characterization results indicated that the two prepared catalyst samples were mesoporous, had a significant number of acidic sites on their surfaces and possessed both inorganic and organic functional groups, making them hybrid solid catalysts. The investigation of the catalytic potential of the two materials revealed that NH_2-MK10-Bpy-Mn was more efficient than MK10-Bpy-Zn for the transesterification of β-keto EAA. The optimization by the Taguchi approach showed that the catalyst loading, butanol: ethyl acetoacetate molar ratio, temperature and time had a significant influence on the transesterification process. A decline in the activities of the catalysts after five transesterification cycles was noticed, indicating that the physisorbed organic molecules were not fully removed during the catalyst recovery stage, which resulted in the loss of active sites. Nevertheless, both catalysts were efficient and should be tested for the conversion of α-keto esters and γ-keto esters as well as other β-keto esters.

Data availability

The authors hereby confirm that the data supporting the findings of this research work are within the manuscript.

Conflicts of interest

There are no conflicts to declare.

Acknowledgements

The support of Belt and Road Innovation Research at Huazhong University of Science and Technology, Wuhan, China through the Talent Exchange Project No. DL2022154006L is highly appreciated by Dr Adeyinka Sikiru Yusuff. Prof. Yanlong Gu is gratefully acknowledged the financial support from the National Key Research and Development Project (2022YFE0124100) and the Innovation and Talent Recruitment Base of New Energy Chemistry and Device (B21003).

References

1 R. K. Sharma and D. Rawat, An efficient and recyclable silica based inorganic-organic hybrid zinc catalyst for transesterification of β-keto ester, *J. Inorg. Organomet. Polym.*, 2011, **21**, 619–626.
2 S. Benetti, R. Romagnoli, C. De Risi, G. Spalluto and V. Zanirato, Mastering beta-keto esters, *Chem. Rev.*, 1995, **9**, 1065.
3 M. C. Hennessy and T. P. O. Sullivan, Recent advances in the transesterification of β-keto ester, *RSC Adv.*, 2021, **11**, 22859.
4 B. P. Bandgar, V. S. Sadavarte and L. S. Uppalla, Zn mediated transesterification of β-keto ester, *J. Chem. Res.*, 2001, 16–17.
5 J. Yang, C. Ji, Y. Zhao, Y. Li, S. Jiang, Z. Zhang, Y. Ji and W. Liu, Unprecedented alkylation of carboxylic acids by boron trifluoride etherate, *Synth. Commun.*, 2010, **40**, 957–963.
6 M. Li, J. Yang and Y. Gu, Manganese chloride as an efficient catalyst for selective transformations of indoles in the presence of a keto carbonyl group, *Adv. Synth. Catal.*, 2011, **353**, 1551–1564.
7 O. Mhasni and F. Rezgui, The first DMAP-mediated palladium-free Tsuji–Trost-type reaction of cyclic and acyclic Baylis–Hillman alcohols with active methylene compounds, *Tetrahedron Lett.*, 2010, **51**, 586–587.
8 S. Shinoda and A. Osuka, Transesterification of the α-keto ester in methyl pheophorbide-*a*, *Tetrahedron Lett.*, 1996, **37**, 4945–4948.
9 N. Inahashi, T. Fujiwara and T. Sato, A simple and efficient method for transesterification of b-keto esters catalyzed by cesium fluoride, *Synlett*, 2008, 605–607.
10 B. Das, P. Thirupathi, I. Mahender, V. S. Reddy and Y. K. Rao, Amberlyst-15: an efficient reusable heterogeneous catalyst for the synthesis of 1,8-dioxo-octahydroxanthenes and 1,8-dioxo-decahydroacridines, *J. Mol. Catal. A: Chem.*, 2006, **247**, 233–239.
11 S. P. Chavan, K. Shivasankar, R. Sivappa and R. Kale, Zinc mediated transesterification of β-ketoesters and coumarin synthesis, *Tetrahedron Lett.*, 2002, **43**, 8583–8586.
12 M. Gohain, V. Kumar, J. H. van Tonder, H. C. Swart, O. M. Ntwaeaborwa and B. C. B. Bezuidenhoudt, Nano $CuFe_2O_4$: an efficient, magnetically separable catalyst for transesterification of β-ketoesters, *RSC Adv.*, 2015, **5**, 18972–18976.
13 B. S. Balaji and B. M. Chanda, Simple and high yielding syntheses of β-keto ester catalyzed by zeolite, *Tetrahedron*, 1998, **54**, 13237–13252.
14 D. Liu, J. H. Lei, L. P. Guo, D. Qu, Y. Li and B. L. Su, One-pot aqueous route to synthesize highly ordered cubic and hexagonal mesoporous carbons from resorcinol and hexamine, *Carbon*, 2012, **50**, 476–487.
15 J. Xu, D. Ma, Y. Chen, Y. Wang and X. Li, *Microporous Mesoporous Mater.*, 2017, **241**, 72–78.
16 C. Anand, S. V. Priya, G. Lawrence, G. P. Mane, D. S. Dhawale, K. S. Prasad, V. V. Balasubramanian, M. A. Wahab and A. Vinu, Transesterification of ethylacetoacetate catalysed by metal free mesoporous carbon nitride, *Catal. Today*, 2013, **204**, 164–169.
17 L. Zatta, J. E. F. Gardolinski and F. Wypych, Raw halloysite as reusable heterogeneous catalyst for esterification of lauric acid, *Appl. Clay Sci.*, 2011, **51**, 165–169.
18 M. A. Olutoye, S. W. Wong, L. H. Chin, S. W. Amani, M. Asif and B. H. Hameed, Synthesis of fatty acid methyl esters via the transesterification of waste cooking oil by methanol with a barium-modified montmorillonite K10 catalyst, *Renewable Energy*, 2016, **86**, 392–398.

19 C. R. Reddy, B. Vijayakumar, P. Iyengar, G. Nagendrappa and B. S. Jai Prakash, Synthesis of phenylacetates using aluminium-exchanged montmorillonite clay catalyst, *J. Mol. Catal. A Chem.*, 2004, **223**, 117–122.

20 S. Chavan, A. Pasupathy, S. Shengule, V. Shinde and A. Ramanathan, *Catalytic Transesterification of -Ketoesters with H-FER under Solvent Free Conditions ARKIVOC*, 2005, pp. 162–168.

21 A. S. Yusuff and M. O. Onobonoje, Biodiesel production from transesterified yellow grease by ZSM-5 zeolite-supported BaO catalyst: process optimization by Taguchi's experimental design approach, *Mater. Renew. Sustain. Energy*, 2023, **12**(3), 199–208.

22 A. S. Yusuff, A. K. Thompson-Yusuff and J. Porwal, Sulfonated biochar catalyst derived from eucalyptus tree shed bark: synthesis, characterization and its evaluation in oleic acid esterification, *RSC Adv.*, 2022, **12**, 10237–10248.

23 H. Amani, Z. Ahmad and B. H. Hameed, Transesterification of waste cooking palm oil by MnZr with supported alumina as a potential heterogeneous catalyst, *J. Ind. Eng. Chem.*, 2014, **20**, 4437–4442.

24 P. Arun, S. M. Pudi and P. Biswas, Acetylation of glycerol over sulfated alumina: reaction parameter study and optimization using response surface methodology, *Energy Fuels*, 2016, **30**, 584–593.

25 U. I. Nda-Umar, I. Ramli, E. N. Muhamad and Y. H. Taufiq-Yap, Synthesis and characterization of sulfonated carbon catalysts derived from biomass waste and its evaluation in glycerol acetylation, *Biomass Convers. Biorefin.*, 2022, **12**(6), 2045–2060.

26 I. Dosuna-Rodríguez, C. Adriany and E. M. Gaigneaux, Glycerol acetylation on sulphated zirconia in mild conditions, *Catal. Today*, 2011, **167**, 56–63.

27 Y. A. B. Neolaka, Z. S. Nagara, Y. Lawa, J. N. Naat, D. P. Benu, A. Chetouani, H. Elmsellem, H. Darmokoesomo and H. S. Kusuma, Simple design and preliminary evaluation of continuous submerged solid small-scale laboratory photoreactor (CS4PR) using TiO_2/NO_3-@TC for dye degradation, *J. Environ. Chem. Eng.*, 2019, **7**(6), 103482.

28 A. Fisli, Y. K. Krisnanandi and J. Gunlazuardi, Preparation and characterization of $Fe_2O_3/SiO_2/TiO_2$ composite for methylene blue removal in water, *Int. J. Technol.*, 2017, **1**, 76–84.

29 A. S. Yusuff, L. T. Popoola, O. D. Adeniyi and M. A. Olutoye, Coal fly ash supported ZnO catalyzed transesterification of Jatropha curcas oil: optimization by response surface methodology, *Energy Convers. Manage.: X*, 2022, **16**, 100302.

30 I. Lawan, Z. N. Garba, W. Zhou, M. Zhang and Z. Yuan, Synergies between the microwave reactor and CaO/zeolite catalyst in waste lard biodiesel production, *Renewable Energy*, 2020, **145**, 2550–2560.

31 A. S. Yusuff, N. B. Ishola, A. O. Gbadmosi, T. M. Azeez and M. O. Onibonoje, An artificial intellignece approach to model and optimize biodiesel production from used cooking oil using CaO incorporated zeolite catalyst, *Energy Convers. Manage.: X*, 2023, **20**, 100452.

32 M. L. Kantam, A. Ravindra, C. V. Reddy, B. Sreedhar and B. M. Choudary, Layered double hydroxides-supported diisopropylamide: synthesis, characterization and application in organic reactions, *Adv. Synth. Catal.*, 2006, **348**, 569–578.

33 Y. H. Tan, M. O. Abdullah, C. Nolasco-Hipolito and Y. H. Taufiq-Yap, Waste ostrich- and chicken-eggshells as heterogeneous base catalyst for biodiesel production from used cooking oil: catalyst characterization and biodiesel yield performance, *Appl. Energy*, 2015, **160**, 58–70.

34 S. M. Ghoreishi and P. Moein, Biodiesel synthesis from waste vegetable oil via transesterification reaction in supercritcal methanol, *J. Supercrit. Fluids*, 2013, **76**, 24–31.

35 K. F. Yee and K. T. Lee, Palm oil as feedstocks for biodiesel production via heterogeneous transesterification: optimization study, *International Conference on Environment 2008 (ICENV 2008)*.

36 A. Giwa, P. O. Nkeonye, K. O. Bello and E. G. Kolawole, Solar photocatalytic degradation of acid blue 29, *J. Chem. Soc. Nigeria*, 2011, **36**(1), 82–89.

37 G. Sathicq, L. Musante, G. Romanelli, G. Pasquale, J. Autino, H. Thomas and P. Vazquez, Transesterification of β-keto esters catalyzed by hybrid materials based on silica-gel, *Catal. Today*, 2008, **133–135**, 455–460.

38 **https://www.chemicalbook.com/ChemicalProductProperty_EN_CB5267181.htm**.